Spectrally Efficient 168 Gb/s/λ WDM 64-QAM Single-Sideband Nyquist-Subcarrier Modulation With Kramers–Kronig Direct-Detection Receivers

Zhe Li, *Student Member, IEEE*, M. Sezer Erkılınç, *Member, IEEE*, Kai Shi, *Member, IEEE*, Eric Sillekens, *Student Member, IEEE*, Lidia Galdino, *Member, IEEE*, Tianhua Xu, *Member, IEEE*, Benn C. Thomsen, *Member, IEEE*, Polina Bayvel, *Fellow, IEEE*, and Robert I. Killey, *Senior Member, IEEE*

(Highly-Scored Paper)

***Abstract*—Due to their simple and cost-effective transceiver architecture, single-polarization and single-photodiode-based direct-detection (DD) systems offer advantages for metropolitan area network and data-center interconnect applications. Single-sideband subcarrier modulation (SSB SCM) signaling with DD has the potential to achieve high information spectral density (ISD) but its performance can be significantly degraded by signal–signal beat interference (SSBI). The recently proposed Kramers–Kronig (KK) digital signal processing scheme is effective in eliminating the SSBI penalty. Through the use of the KK scheme, we achieved 4 × 168 Gb/s wavelength division multiplexing DD SSB 64-QAM Nyquist-SCM signal transmission over 80 km of uncompensated standard single-mode fiber at a net ISD of up to 4.61 (b/s)/Hz. The joint optimization of the optical carrier-to-signal power ratio and the KK algorithm sampling rate is described.**

***Index Terms*—Data center interconnect, digital linearization, direct detection, Kramers–Kronig receiver, metro networks, Nyquist-pulse shaped subcarrier modulation, receiver-based electronic dispersion compensation, signal–signal beat interference, spectrally efficient wavelength division multiplexing.**

I. Introduction

IT IS widely recognized that the unprecedented traffic growth in metropolitan area networks, mobile back-haul and inter-data center links will require optical fiber transmission systems which offer high capacity, spectrally-efficient signaling with tolerance to transmission impairments, using optical transceivers which are compact, low power and low cost and operate over link lengths of at least 80 km [1]. In comparison to dual-polarization coherent transceivers [2], [3], which require multiple balanced detectors and analog-to-digital converters (ADCs), optical hybrids, a local oscillator laser and polarization beam splitters and combiners, single-polarization and single-photodiode based direct-detection (DD) transceivers may be favorable for these applications due to their simple and low-cost optical hardware structure. Alongside other modulation formats, such as discrete multi-tone (DMT) [4], [5], and carrierless amplitude and phase (CAP) modulation [6], single-sideband (SSB) quadrature amplitude modulation (QAM) subcarrier modulation (SCM) is a promising signal format for DD transceivers. In contrast to double sideband (DSB) signaling, SSB signaling avoids dispersion induced power fading [7] and, at the same time, increases the achievable optical information spectral density (ISD) [8], [9]. A drawback of the SSB SCM direct detection scheme is that the signal-signal beat interference (SSBI) generated by square-law detection causes a significant degradation in its performance [10]. Therefore, in order to make such systems capable of transmitting high data rate (≥100 Gb/s/λ) and spectrally-efficient (≥3 (b/s)/Hz) payloads over typical medium reach links of up to ∼80 km (e.g., metro networks and data-center interconnects), it is necessary to implement techniques that can reduce or eliminate this impairment.

To overcome the problem of SSBI, a number of effective digital compensation techniques have been demonstrated for SSB SCM DD transceivers [11]–[19]. The general principle of these is to treat the signal-signal beating terms as perturbations to the signal, which can be calculated from the received signal waveform and then subtracted from it. However, optimum transceiver performance has not yet been achieved with such approaches. The recently proposed Kramers-Kronig (KK) digital scheme [20], [21] is an alternative method of carrying out linearization. By accurately recovering the optical phase of the transmitted signal from its detected amplitude, through the use of the KK relationship, this scheme directly reconstructs the complex waveform of the detected optical signal and hence avoids the nonlinear beating interference introduced by square-law detection. Simulations and experiments have shown that the KK scheme offers outstanding performance and makes DD

Manuscript received October 23, 2017; revised December 4, 2017; accepted December 13, 2017. Date of publication December 26, 2017; date of current version March 1, 2018. This work was supported by the UK EPSRC UNLOC EP/J017582/1 project. *(Corresponding author: Zhe Li.)*

Z. Li, M. S. Erkılınç, E. Sillekens, L. Galdino, P. Bayvel, and R. I. Killey are with the Optical Networks Group, Department of Electronic & Electrical Engineering, University College London, London WC1E 7JE, U.K. (e-mail: zhe.li@ee.ucl.ac.uk; m.erkilinc@ee.ucl.ac.uk; e.sillekens@ee.ucl.ac.uk; l.galdino@ee.ucl.ac.uk; p.bayvel@ucl.ac.uk; r.killey@ucl.ac.uk).

K. Shi and B. C. Thomsen are with the Microsoft Research Ltd, Cambridge CB1 2FB, U.K. (e-mail: t-kashi@microsoft.com; benn.thomsen@microsoft.com).

T. Xu is with the School of Engineering, University of Warwick, Coventry CV4 7AL, U.K. (e-mail: tianhua.xu@warwick.ac.uk).

Color versions of one or more of the figures in this paper are available online at http://ieeexplore.ieee.org.

Digital Object Identifier 10.1109/JLT.2017.2785858

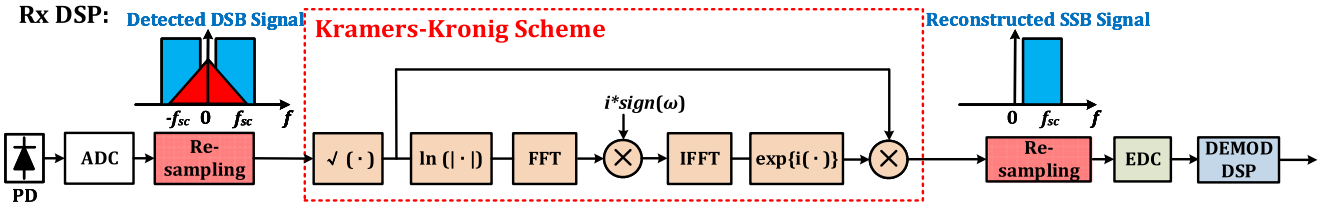

Fig. 1. Receiver DSP using the Kramers-Kronig scheme and Rx-EDC. PD: Photodiode. ADC: analogue-to-digital converter. EDC: electronic dispersion compensation. DEMOD DSP: Conventional demodulation DSP for SSB SCM signal.

transceivers capable of supporting high capacity transmission over 80 km or more of uncompensated standard single-mode fiber (SSMF) [12], [22]–[27].

In this paper, we explore the achievable ISD limits of single-polarization, single-photodiode direct-detection transceivers employing the KK scheme, through experiments with a high-order QAM format and ultra-dense wavelength division multiplexing (WDM). We successfully transmitted 35 GHz-spaced 4 × 168 Gb/s WDM SSB 64-QAM Nyquist subcarrier modulation (Nyquist-SCM) signals [28]–[31] to achieve 4.61 (b/s)/Hz net ISD over 80 km. All experiments employed uncompensated SSMF, since the KK scheme enables effective electronic dispersion compensation at the receiver as well [12]. This paper is an extension of the work presented in [32], with further in-depth descriptions of the experiments and additional experimental results. Moreover, we also investigate some of the key aspects of the KK scheme's practical implementation, namely the joint optimization of the optical carrier-to-signal power ratio (CSPR) at the transmitter and the resampling rate in the Kramers-Kronig algorithm within the receiver, extending the study in [33] to 64-QAM.

II. Principle of Operation

Fig. 1 shows the structure of the Kramers-Kronig direct-detection receiver. A single photodiode carries out optical-to-electrical conversion, and this process of envelope detection removes the optical phase, resulting in a DSB electrical signal. Following this, the signal is digitized and then passed to the Kramers-Kronig algorithm. The purpose of the KK scheme is to calculate the phase of the transmitted optical signal from its amplitude, using the Kramers-Kronig relationship [20], [34]. Provided the transmitted signal fulfils the minimum phase condition (i.e., the optical carrier has an amplitude larger than that of the signal), and is single-sideband, the optical phase of the transmitted SSB signal, $\varphi(n)$, can be accurately calculated from its detected intensity, $h(n)$. Therefore, the complex-valued waveform of the transmitted SSB signal before the square-law detection, $V_{KK}(n)$, can be fully reconstructed. The mathematical expressions of the KK scheme are described in (1)–(3):

$$h(n) = \sqrt{V_{DD}(n)}. \tag{1}$$

$$\varphi(n) = \mathcal{F}^{-1}\left\{i\, sign(\omega)\, \mathcal{F}\left\{ln\left[|h(n)|\right]\right\}\right\}. \tag{2}$$

$$V_{KK}(n) = h(n) \cdot exp\left\{i\varphi(n)\right\}. \tag{3}$$

where $V_{DD}(n)$ is the detected real-valued (and hence DSB) signal, n is the discrete time index, $sign(\omega)$ is the sign function, which is equal to 1 for $\omega > 0$, to 0 for $\omega = 0$, and to -1 for $\omega < 0$, $\mathcal{F}\{\bullet\}$ and $\mathcal{F}^{-1}\{\bullet\}$ are the Fourier and inverse Fourier transform operators. Note that, since the KK scheme includes the nonlinear square-root and logarithm calculations, which cause signal spectral broadening, it is necessary for the KK algorithm to be carried out at a relatively high sampling rate.

Two key conditions need to be simultaneously fulfilled in order to ensure that the KK scheme achieves the optimum performance. Firstly, at the transmitter, a sufficiently high power optical carrier must be added to the SSB signal (i.e., a sufficiently high optical carrier-to-signal power ratio value must be used) to ensure minimum phase signaling. Secondly, at the receiver, a sufficiently high sampling rate should be used for the KK algorithm, to handle the signal's bandwidth increase caused by the nonlinear functions (logarithm and square-root). Hence upsampling and downsampling are performed before and after, respectively, the KK block.

Following the KK scheme, electronic dispersion compensation (EDC) is carried out. As discussed in [12], [20], since beating interference is effectively suppressed by the KK scheme, the receiver-based EDC achieves similar performance to that of the transmitter-based EDC, and at the same time simplifies system operation, since information about the link dispersion is not required at the transmitter.

III. Experimental Setup

As described in the previous section, due to the outstanding performance of the KK DD receiver, we utilized such a receiver to experimentally explore the achievable ISD limits of single-polarization SSB Nyquist-SCM DD systems. The transmission testbed is shown in Fig. 2. Odd- and even-indexed WDM channels were first generated using a pair of IQ-modulators seeded by four external cacity lasers (ECLs). The IQ-modulators were driven by two 92 GSa/s arbitrary waveform generators (AWGs) with a 3-dB bandwidth of 33 GHz. In the transmitter DSP (Tx DSP), a 28 GBd (gross bit rate of 168 Gb/s) SSB 64-QAM Nyquist-SCM signal was generated. The subcarrier frequency was set to 14.28 GHz (0.51 × symbol rate) and the root-raised-cosine filters used for Nyquist pulse-shaping had a 1% roll-off factor, resulting in a guard band between the signal and the optical carrier of only 140 MHz. By biasing the IQ-modulators above the null point, an optical carrier was generated, with the bias voltages manually adjusted to obtain the desired optical CSPR values. Following this, the four de-correlated channels

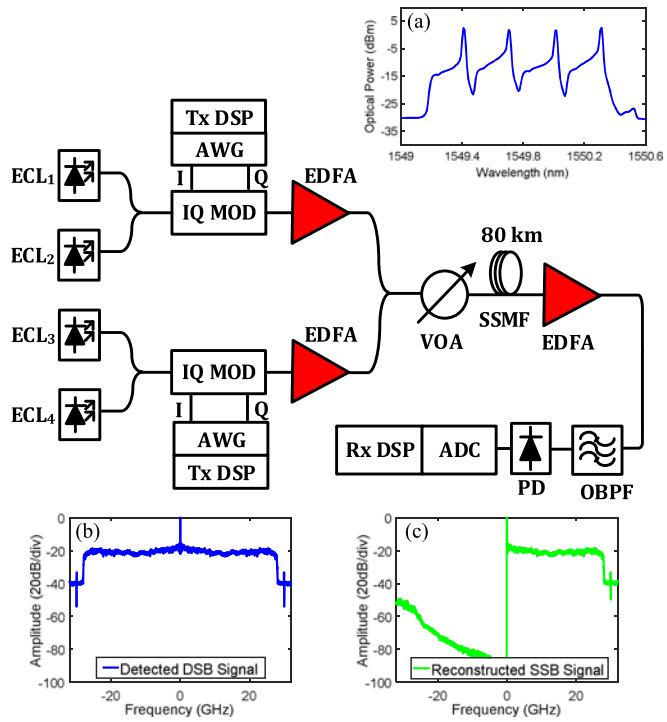

Fig. 2. Optical transmission experimental testbed. Insets: (a) experimental transmitted WDM spectrum. (b) detected digital DSB signal and (c) reconstructed digital SSB signal spectrum obtained using the KK scheme. ECL: External cavity laser. AWG: Arbitrary waveform generator. EDFA: Erbium-doped fiber amplifier. VOA: Variable optical attenuator. SSMF: Standard single-mode fiber. OBPF: Optical band-pass filter. PD: Photodiode.

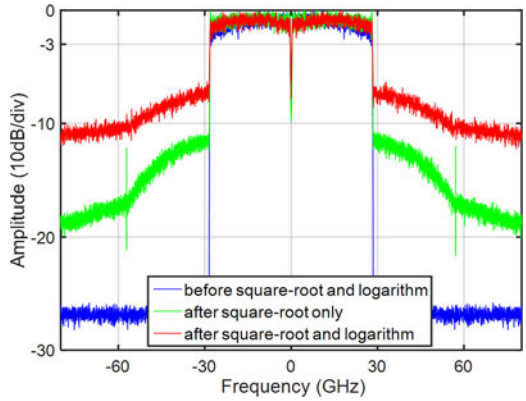

Fig. 3. Detected digital DSB signal before (blue) and after (green) square-root only, (red) square-root and logarithm operations.

were wavelength multiplexed, with the WDM channel spacing set to 35 GHz, giving a gross optical ISD of 4.8 (b/s)/Hz. The transmitted WDM signal's spectrum is shown in Fig. 2 inset (a). Note that, since the optical CSPR is a crucial parameter for the performance of SSB DD system, it needs to be optimized for each value of the optical signal-to-noise ratio (OSNR). A uniform CSPR across all the channels was achieved. The transmission experiments were performed using an 80 km single-span SSMF followed by an Erbium-doped fiber amplifier (EDFA) with a noise figure of 5 dB.

At the receiver, a flat-topped optical band-pass filter (OBPF) with 31 GHz FWHM and a filter edge gradient of 800 dB/nm was used to select the WDM channel of interest (and to emulate the wavelength demultiplexer). A single PIN photodiode (PD) with 40 GHz 3-dB bandwidth and a single ADC operating at 80 GSa/s were utilized to perform signal detection and digitization. The received optical signal power was 1 dBm, which is within the optimum operation range of the photodiode. The detected signal's spectrum after analog-to-digital conversion is shown in Fig. 2 inset (b). Note that, as the optical phase information is lost, the signal after detection is real-valued and double-sideband. In the receiver DSP (Rx DSP), before entering the KK block, the detected signal was first resampled from the ADC rate (80 GSa/s) to a value of between 2 and 7 Sa/symbol (56 GSa/s to 196 GSa/s). The reconstructed SSB signal's spectrum is plotted in Fig. 2 inset (c). Following this, the signal was resampled to 2.5 Sa/symbol, and EDC and 64-QAM Nyquist-SCM demodulation were performed (details of the SSB QAM Nyquist-SCM modulation and demodulation can be found in [9]). Finally, BER was measured by error counting over 2^{20} bits.

The effectiveness of the KK scheme was compared with two alternative linearization schemes: the single-stage linearization filter [11], and the two-stage linearization filter [12]. Both compensation schemes work by calculating the signal-signal beating terms from the detected signal waveform and subtracting these reconstructed terms from the detected signal. The single-stage linearization filter has a very simple DSP structure and the two-stage linearization filter offers an improvement in performance over the single-stage filter. The choice of schemes provides a trade-off between complexity and performance [12].

IV. Experimental Results

Both the optical back-to-back and WDM transmission evaluations were carried out with the experimental testbed shown in Fig. 2. The optical CSPR value at the transmitter and the resampling rate in the KK DSP at the receiver were jointly adjusted.

A. Back-to-Back Performance Evaluation

A higher sampling rate is required by the Kramers-Kronig algorithm to accurately represent the signals which are broadened by the square-root and logarithm operations (Fig. 1), according to the Nyquist Theorem. Plots of the digital signal spectra before and after the square-root and logarithm operations are shown in Fig. 3, from which the spectral broadening can be observed. As a result of the square-root and logarithm operations, the -3 dB and -10 dB bandwidths of the signal were found to be 28.3 GHz and 60.6 GHz respectively. One of the aims of the back-to-back performance evaluation was to quantify the required resampling rate.

The optical back-to-back performance was assessed by performing amplified spontaneous emission (ASE)-noise loading at the receiver. The required OSNR at the 20% FEC threshold (assumed to be BER $= 1.5 \times 10^{-2}$ [35]) versus CSPR for a range of resampling rates used for the KK algorithm is plotted

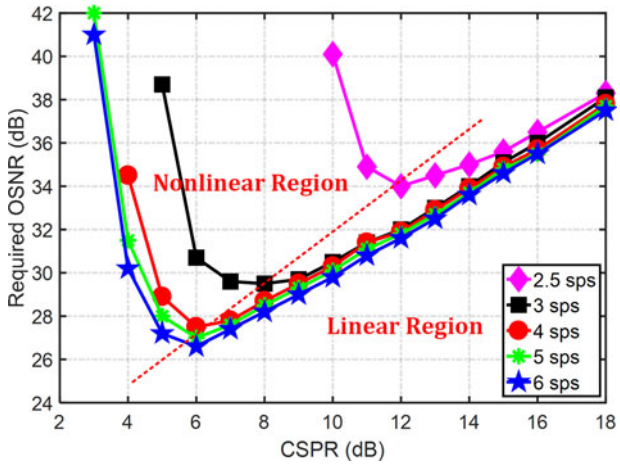

Fig. 4. Required OSNR at BER $= 1.5 \times 10^{-2}$ versus CSPR at different KK scheme resampling rates.

in Fig. 4. It can be observed that the optimum CSPR value (resulting in the minimum required OSNR) is dependent on the resampling rate. When the system operates at CSPRs above the optimum, the excessive power of the optical carrier (which is included in the numerator of the OSNR calculation), results in higher required OSNRs at the fixed BER threshold. At CSPR values below the optimum, since the minimum phase condition is not fulfilled, the KK scheme fails to accurately reconstruct the transmitted optical SSB signal and hence the system suffers from large nonlinear penalties. Regarding the variation in the system's performance with different resampling rates, the value of the required OSNR at the optimum CSPR value was found to increase when the KK algorithm was performed at the lower sampling rates. Distortion due to aliasing increases, affecting the trade-off between nonlinear distortion and excessive optical carrier power, and resulting in the optimum CSPR value shifting to higher values at lower resampling rates (from 6 dB at 6 Sa/symbol to 12 dB at 2.5 Sa/symbol).

The sensitivity of the KK scheme's performance towards variations of the sampling rate was also compared with that of other digital linearization schemes. The required OSNR values at the optimum CSPR values over a range of sampling rates for the case without linearization, and for the cases with the KK scheme, the single-stage linearization filter [11], and the two-stage linearization filter [12], are plotted in Fig. 5(a). With the KK scheme, when the resampling rate was below 4 Sa/symbol (112 GSa/s), we observed a significant increase in the required OSNR (from 27.5 dB at 4 Sa/symbol to 40.1 dB at 2.3 Sa/symbol). The value of the required OSNR with the KK scheme converged asymptotically to 26.7 dB when it was operating at 6 Sa/symbol (168 GSa/s) or higher. In contrast to the KK scheme, convergence to the optimum value was observed at lower sampling rates for the systems with the single-stage and the two-stage linearization filters. This is because, unlike with the KK scheme, these two linearization filtering schemes do not include calculations which lead to signal broadening, and thus work well at lower sampling rates. At resampling rates lower than 2.5 Sa/symbol, the performance of both linearization filters surpassed that of the KK scheme. However, the required OSNR values converged to higher values (38.5 dB without linearization, 33.5 dB with the single-stage linearization filter and 31.2 dB with the two-stage linearization filter) than with the KK scheme.

Fig. 5(b) presents the BER versus OSNR with different resampling rates, with the CSPR value optimized at each OSNR level. The experimental results were compared with those from simulations (dotted line in Fig. 5(b)) using the KK scheme operating at 6 Sa/symbol, assuming transceivers using ideal electrical and optical components, *i.e.*, no quantization or other electrical noise, linear IQ modulator and an ideal rectangular-shaped optical bandpass filter. The experimental required OSNR at the 1.5×10^{-2} pre-FEC BER threshold was found to be 38.3 dB without using receiver linearization, reducing by 11.6 dB to 26.7 dB with the KK scheme operating at 6 Sa/symbol. The BER at 36 dB OSNR was decreased by more than one order of magnitude, from 2.1×10^{-2} without linearization to 1.5×10^{-3} with the KK scheme (at 6 Sa/symbol). The corresponding optimum CSPR value reduced from 14 dB without linearization to 9 dB with the KK scheme. The received signal constellations at an OSNR of 36 dB with the KK scheme operating at four different resampling rates are plotted in Fig. 5 insets (I)–(IV). The error-vector magnitude (EVM) reduced from 13.8% at 2.5 Sa/symbol to 8.9% at 6 Sa/symbol. In comparison to the theoretical curve obtained from ideal system simulations, there was a 2.9 dB difference at the FEC threshold, with an error floor at BER of 1.3×10^{-3}, which can be explained by the transceiver's electrical and quantization noise, which were not included in the simulation.

B. WDM Transmission Performance Evaluation

Following the back-to-back characterization of the transceiver, the WDM transmission performance over 80 km of uncompensated SSMF was evaluated. The BER at the optimum launch power is plotted versus CSPR for different KK algorithm sampling rates (Fig. 6(a)). As in the case of back-to-back operation, the trade-off between nonlinear distortion and excessive optical carrier power can be observed. When operating at lower sampling rates, the KK scheme's performance was reduced, and the optimum CSPR shifted to higher values (from 10 dB at 6 Sa/symbol sampling rate for the KK algorithm to 15 dB at 2.5 Sa/symbol). Note that the higher optimum CSPR values in this transmission experiment compared to those in the back-to-back experiment (Fig. 4) are due to the OSNR values being higher, since no ASE noise loading was applied in this case. In Fig. 6(b), BERs measured at optimum launch powers and optimum CSPRs are plotted as a function of sampling rate for the cases without linearization, with the KK scheme, and with the single-stage and two-stage linearization filters. It can be seen that, as the resampling rate was varied from 2 to 4 Sa/symbol, the BER with the KK scheme dramatically decreased. For resampling rates of 6 Sa/symbol and above, the BER of the KK scheme converged to 4.5×10^{-3}. In contrast, the effectiveness of both receiver linearization filters showed less dependence on the sampling rate, and they provided better performance at

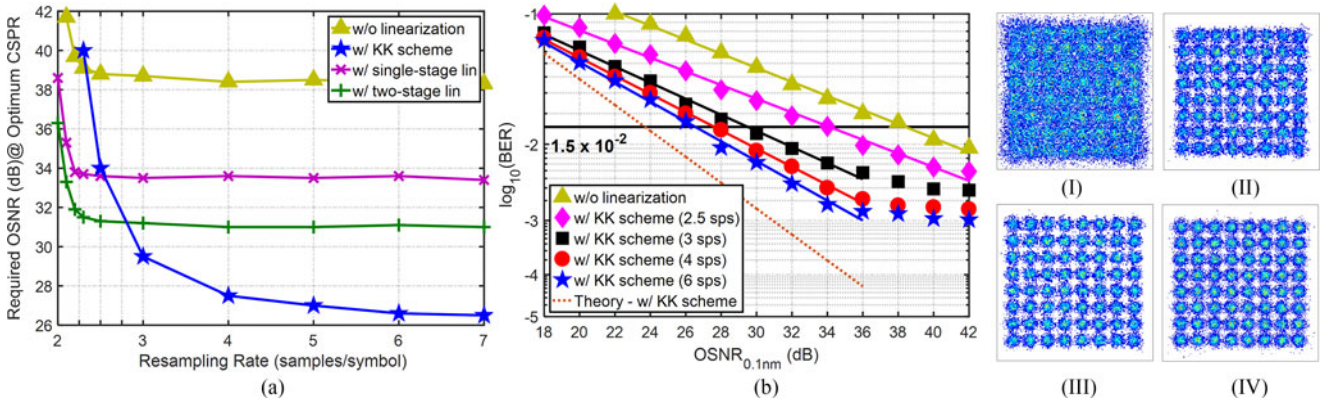

Fig. 5. (a) Required OSNR (assuming BER $= 1.5 \times 10^{-2}$) at the optimum CSPR value versus resampling rate for the cases of without and with the KK scheme, the single-stage linearization filter, and the two-stage linearization filter. (b) BER versus OSNR at different KK scheme resampling rates. Insets: Received signal constellations at 36 dB OSNR with the KK scheme operating at (I) 2.5 Sa/symbol (EVM = 13.8%), (II) 3 Sa/symbol (EVM = 11.3%), (III) 4 Sa/symbol (EVM = 9.7%), and (IV) 6 Sa/symbol. (EVM = 8.9%).

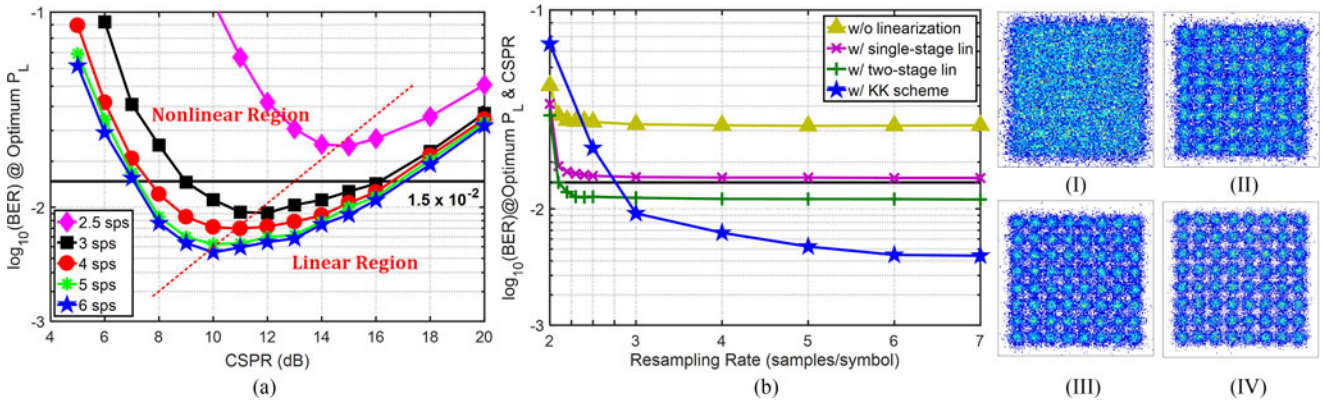

Fig. 6. System transmission performance with the KK scheme: (a) BER at the optimum launch power versus CSPR at 80 km at different KK scheme resampling rate. (b) BER at the optimum launch power versus resampling rate at 80 km for the cases of without and with the KK scheme, the single-stage linearization filter, and the two-stage linearization filter. Insets: Received signal constellations at 80 km with the KK scheme operating at (I) 2.5 Sa/symbol (EVM = 17.7%), (II) 3 Sa/symbol (EVM = 13.1%), (III) 4 Sa/symbol (EVM = 11.1%), and (IV) 6 Sa/symbol (EVM = 10.1%).

sampling rates below 2.5 Sa/symbol. However, the minimum BER values (1.6×10^{-2} and 1.1×10^{-2} with single-stage and two-stage linearization filters, respectively) were higher than that obtained with the KK scheme operating at the optimum sampling rate.

The BERs with respect to optical launch power per channel without and with the digital linearization schemes for WDM transmission over 80 km are plotted in Fig. 7. Note that the launch power includes the optical carrier and the 64-QAM signal. It can be seen that the KK transceiver (with 6 Sa/symbol) had an optimum power of approximately 2 dBm, 1 dB below the values with single-stage and two-stage linearization filters. Furthermore, the BER value were measured for all four WDM channels after transmission over 80 km and using the KK scheme (at 6 Sa/symbol), and the linearization filters (at 2.5 Sa/symbol) (Fig. 8). The average BER value across the channels using the KK scheme was 4.1×10^{-3}. Assuming the standard 20% FEC overhead, the net ISD was 4.0 (b/s)/Hz. However, considering the theoretical hard-decision decoding bound for the binary symmetric channel [36], this pre-FEC BER of 4.1×10^{-3} results in a theoretical net ISD upper bound of 4.61 (b/s)/Hz. This exceeds the previous record of 3.58 (b/s)/Hz [37] for this distance, which was achieved by employing SSB PAM-8 with Volterra equalization. Additionally, instead of performing EDC pre-compensation at the transmitter (requiring feedback between receiver and transmitter, and an accurate knowledge of the link dispersion at the transmitter), the KK scheme also enables the utilization of EDC at the receiver without sacrificing performance, leading to simpler system operation.

As high oversampling rates lead to increased DSP complexity, the sampling rate utilized in practical implementations of the KK scheme may be lower than the theoretical optimum value of 6 Sa/symbol. Note that, unlike with homodyne receivers in which the real and imaginary parts of the signal are detected separately with two ADCs, and the minimum required sampling rate per ADC is 1 Sa/symbol, in the SSB subcarrier modulation scheme (as with coherent heterodyne receivers) the whole complex field of the signal is reconstructed from the output of a single ADC, and the theoretical minimum sampling rate required to represent the signal is 2 Sa/symbol. Hence, the optimum

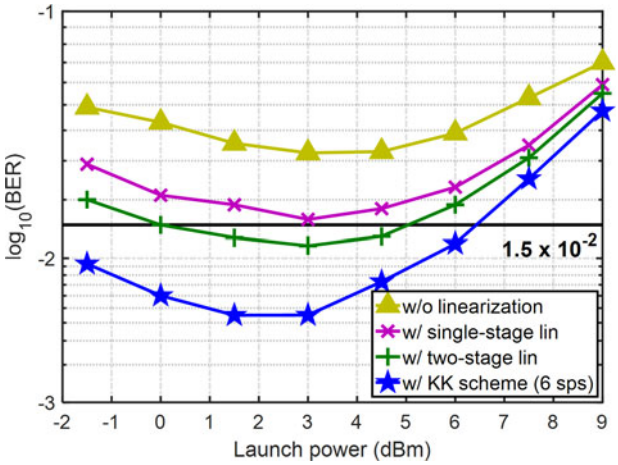

Fig. 7. BER versus optical launch power per channel after 80 km transmission for the cases without and with the KK scheme (6 Sa/symbol), the single-stage linearization filter, and the two-stage linearization filter.

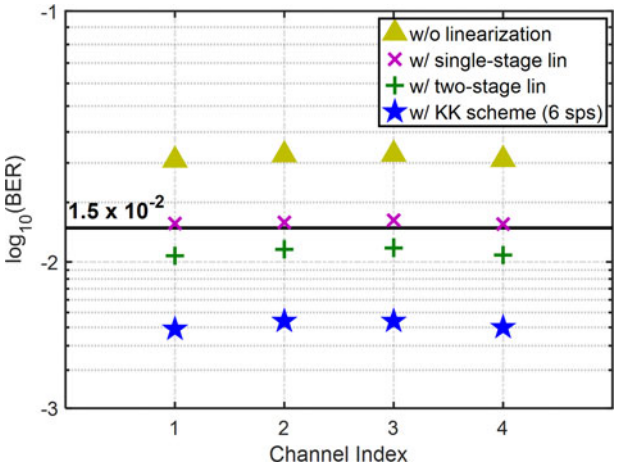

Fig. 8. BER for each WDM channel after 80 km transmission for the cases without and with the KK scheme (6 Sa/symbol), the single-stage linearization filter, and the two-stage linearization filter.

sampling rate of 6 Sa/symbol required by the KK algorithm represents 3-fold digital oversampling. Further analysis will be required to calculate the computational complexity of the KK scheme.

V. Conclusion

The use of single-polarization and single-photodiode based direct-detection (DD) receivers is attractive for short- and medium-haul links, such as those in metro networks and between data-centers, due to their simple and low-cost optical hardware structure. We reported an experimental investigation of 35 GHz-spaced 4 × 168 Gb/s/λ WDM single-sideband 64-QAM Nyquist-subcarrier modulation signaling with Kramers-Kronig direct-detection receivers, operating back-to-back and in transmission over 80 km of uncompensated standard single-mode fiber. As part of the assessment, the joint optimization of the optical carrier-to-signal power ratio (CSPR) and the sampling rate used for the KK algorithm was experimentally studied. Due to the effective receiver linearization achieved using the KK scheme, a net information spectral density of 4.0 (b/s)/Hz (assuming a 20% FEC overhead), and an upper bound on the net ISD of 4.61 (b/s)/Hz (assuming hard-decision FEC) were demonstrated at this distance. The sensitivity of the KK scheme's performance to the sampling rate was compared with alternative recently proposed single-stage and two-stage linearization filters. Both the back-to-back and transmission evaluations indicated that, of the three schemes, the best performance was achieved using the KK scheme (provided a sampling rate corresponding to at least 2.75 Sa/symbol was used for the KK algorithm), with optimum performance being achieved at ≥6 Sa/symbol. This experimental analysis has quantified the trade-off between the linearization performance and the DSP sampling rate in high spectral efficiency 64-QAM direct detection receivers.

References

[1] Q. Zhang, N. Stojanovic, C. Xie, C. Prodaniuc, and P. Laskowski, "Transmission of single lane 128 Gbit/s PAM-4 signals over an 80 km SSMF link, enabled by DDMZM aided dispersion pre-compensation," *Opt. Express*, vol. 24, no. 21, pp. 24580–24591, 2016.

[2] K. Kikuchi, "Fundamentals of coherent optical fiber communications," *J. Lightw. Technol.*, vol. 34, no. 1, pp. 157–179, Jan. 2016.

[3] E. Ip, A. P. T. Lau, D. J. F. Barros, and J. M. Kahn, "Coherent detection in optical fiber systems," *Opt. Express*, vol. 16, no. 2, pp. 753–791, 2008.

[4] H. Yamazaki *et al.*, "300-Gbps discrete multi-tone transmission using digital-preprocessed analog-multiplexed DAC with halved clock frequency and suppressed image," in *Proc. 42nd Eur. Conf. Opt. Commun.*, 2016, paper Th.3.B.4.

[5] Y. Wang, J. Yu, H.-C. Chien, X. Li, and N. Chi, "Transmission and direct detection of 300-Gbps DFT-S OFDM signals based on O-ISB modulation with joint image-cancellation and nonlinearity-mitigation," in *Proc. 42nd Eur. Conf. Opt. Commun.*, 2016, paper 827-829.

[6] J. Wei, N. Eiselt, C. Sánchez, R. Du, and H. Griesser, "56 Gb/s multi-band CAP for data center interconnects up to an 80 km SMF," *Opt. Lett.*, vol. 41, no. 12, pp. 2767–2770, 2016.

[7] H.-Y. Chen, N. Kaneda, J. Lee, J. Chen, and Y.-K. Chen, "Optical filter requirements in an EML-based single-sideband PAM4 intensity-modulation and direct-detection transmission system," *Opt. Express*, vol. 25, no. 6, pp. 5852–5860, 2017.

[8] W.-R. Peng *et al.*, "Theoretical and experimental investigations of direct-detected RF-tone-assisted optical OFDM systems," *J. Lightw. Technol.*, vol. 27, no. 10, pp. 1332–1339, May 2007.

[9] M. S. Erkılınç *et al.*, "Spectrally-efficient WDM Nyquist-pulse-shaped 16-QAM subcarrier modulation transmission with direct detection," *J. Lightw. Technol.*, vol. 33, no. 15, pp. 3147–3155, Aug. 2015.

[10] A. J. Lowery, "Amplified-spontaneous noise limit of optical OFDM lightwave systems," *Opt. Express*, vol. 16, no. 2, pp. 860–865, 2008.

[11] S. Randel, D. Pilori, S. Chandrasekhar, G. Raybon, and P. Winzer, "100-Gb/s discrete-multitone transmission over 80-km SSMF using single-sideband modulation with novel interference-cancellation scheme," in *Proc. Eur. Conf. Opt. Commun.*, 2015, paper Mo.4.5.2.

[12] Z. Li *et al.*, "SSBI mitigation and Kramer-Kronig scheme in single-sideband direct-detection transmission with receiver-based electronic dispersion compensation," *J. Lightw. Technol.*, vol. 35, no. 10, pp. 1887–1893, May 2017.

[13] K. Zou, Y. Zhu, F. Zhang, and Z. Chen, "Spectrally efficient terabit optical transmission with Nyquist 64-QAM half-cycle subcarrier modulation and direct-detection," *Opt. Lett.*, vol. 41, no. 12, pp. 2767–2770, 2016.

[14] Y. Zhu, K. Zou, and F. Zhang, "C-band 112 Gb/s Nyquist single-sideband direct detection over 960 km SSMF," *IEEE Photon. Technol. Lett.*, vol. 29, no. 8, pp. 651–654, Apr. 2017.

[15] W. Peng *et al.*, "Spectrally efficient direct-detected OFDM transmission employing an iterative estimation and cancellation technique," *Opt. Express*, vol. 17, no. 11, pp. 9099–9111, 2009.

[16] C. Sánchez, B. Ortega, and J. Capmany, "System performance enhancement with pre-distorted OOFDM signal waveforms in IM/DD systems," *Opt. Express*, vol. 22, no. 6, pp. 7269–7283, 2014.

[17] C. Ju, X. Chen, N. Liu, and L. Wang, "SSII cancellation in 40 Gbps VSB-IMDD OFDM system based on symbol pre-distortion," in *Proc. Eur. Conf. Opt. Commun.*, 2014, paper P.7.9.
[18] C. Ju, N. Liu, and X. Chen, "Comparison of iteration interference cancellation and symbol predistortion algorithm for direct detection orthogonal frequency division multiplexing passive optical network," *Opt. Eng.*, vol. 54, no. 8, 2015, Art. no. 0861014.
[19] H. Shi, P. Yang, C. Ju, X. Chen, J. Bei, and R. Hui, "SSBI cancellation based on time diversity reception in SSB-DD-OOFDM transmission systems," in *Proc. Conf. Lasers Electro-Opt.*, 2014, paper JTh2A.14.
[20] A. Mecozzi, C. Antonelli, and M. Shtaif, "Kramers-Kronig coherent receiver," *Optica*, vol. 3, no. 11, pp. 1220–1227, 2016.
[21] C. Antonelli, A. Mecozzi, and M. Shtaif, "Kramers-Kronig PAM transceiver," in *Proc. Opt. Fiber Commun. Conf. Exhib.*, 2017, paper Tu3I.5.
[22] X. Chen *et al.*, "218-Gb/s single-wavelength, single-polarization, single-photodiode transmission over 125-km of standard single-mode fiber using Kramers-Kronig detection," in *Proc. Opt. Fiber Commun. Conf. Exhib.*, 2017, paper Th5B.6.
[23] Z. Li *et al.*, "Digital linearization of direct-detection transceivers for spectrally-efficient 100 Gb/s/λ WDM metro networking," *J. Lightw. Technol.*, to be published.
[24] X. Chen *et al.*, "4 × 240 Gb/s dense WDM and PDM Kramers-Kronig detection with 125-km SSMF transmission," in *Proc. Eur. Conf. Opt. Commun.*, 2017, paper W.2.D.4.
[25] S. Fan *et al.*, "Twin-SSB direct detection transmission over 80 km SSMF using Kramers-Kronig receiver," in *Proc. Eur. Conf. Opt. Commun.*, 2017, paper W.2.D.5.
[26] S. T. Le *et al.*, "8 × 256 Gbps virtual carrier assisted WDM direct-detection transmission over a single span of 200 km," in *Proc. Eur. Conf. Opt. Commun.*, 2017, paper Th.PDP.B.1.
[27] X. Chen *et al.*, "Single-wavelength, single-polarization, single photodiode Kramers-Kronig detection of 440-Gb/s entropy-loaded discrete multitone modulation transmitted over 100-km SSMF," in *Proc. Annu. Conf. IEEE Photon. Soc.*, 2017, paper PD1.
[28] A. O. Wiberg, B.-E. Olsson, and P. A. Andrekson, "Single cycle subcarrier modulation," in *Proc. Conf. Opt. Fiber Commun.*, 2009, paper OTuE.1.
[29] J. C. Cartledge and A. S. Karar, "100 Gb/s intensity modulation and direct detection," *J. Lightw. Technol.*, vol. 32, no. 16, pp. 2809–2814, Aug. 2014.
[30] K. Zhong *et al.*, "Experimental demonstration of 608 Gbit/s short reach transmission employing half-cycle 16QAM Nyquist-SCM signal and direct detection with 25 Gbps EML," *Opt. Express*, vol. 24, no. 22, pp. 25057–25067, 2016.
[31] Y. Gao, J. C. Cartledge, A. S. Kashi, S. S.-H. Yam, and Y. Matsui, "Direct modulation of a laser using 112 Gb/s 16-QAM Nyquist subcarrier modulation," *IEEE Photon. Technol. Lett.*, vol. 29, no. 1, pp. 35–38, Jan. 2017.
[32] Z. Li *et al.*, "168 Gb/s/λ direct-detection 64-QAM SSB Nyquist-SCM transmission over 80 km uncompensated SSMF at 4.54 b/s/Hz net ISD using a Kramers-Kronig receiver," in *Proc. Eur. Conf. Opt. Commun.*, 2017, paper Tu.2.E.1.
[33] Z. Li *et al.*, "Joint optimisation of resampling rate and carrier-to-signal power ratio in direct-detection Kramers-Kronig receivers," in *Proc. Eur. Conf. Opt. Commun.*, 2017, paper W.2.D.3.
[34] H. Voelcker, "Demodulation of single-sideband signals via envelope detection," *IEEE Trans. Commun. Technol.* vol. 14, no. 1, pp. 22–30, Feb. 1966.
[35] L. M. Zhang and F. R. Kschischang, "Staircase codes with 6% to 33% overhead," *J. Lightw. Technol.*, vol. 32, no. 10, pp. 1999–2002, May 2014.
[36] C. E. Shannon, "A mathematical theory of communication," *Bell Syst. Tech. J.*, vol. 27, no. 3, pp. 379–423, 1948.
[37] R. Hirai, N. Kikuchi, and T. Fukui, "High-spectral efficiency DWDM transmission of 100-Gbit/s/lambda IM/DD single sideband-baseband-Nyquist-PAM8 signals," in *Proc. Conf. Opt. Fiber Commun.*, 2017, paper Th3D.4.

Authors' biographies not available at the time of publication.